



Letter

Dielectric properties of Cu substituted $\text{Ni}_{0.5-x}\text{Zn}_{0.3}\text{Mg}_{0.2}\text{Fe}_2\text{O}_4$ ferritesM.R. Bhandare^a, H.V. Jamadar^b, A.T. Pathan^b, B.K. Chougale^b, A.M. Shaikh^{c,*}^a Department of Physics, S. M. Joshi College, Pune 411028, MS, India^b Department of Physics, Shivaji University, Kolhapur, 416004 MS, India^c Department of Electronics, The New College, Kolhapur, 416012 MS, India

ARTICLE INFO

Article history:

Received 10 April 2010

Received in revised form

23 November 2010

Accepted 25 November 2010

Available online 3 December 2010

Keywords:

Spinel ferrites

Lattice parameter

Dielectric properties

ac conductivity

ABSTRACT

Dielectric properties of Cu substituted Ni–Zn–Mg ferrite samples having the general formula $\text{Ni}_{0.5-x}\text{Cu}_x\text{Zn}_{0.3}\text{Mg}_{0.2}\text{Fe}_2\text{O}_4$ (where $x = 0.0, 0.1, 0.2, 0.3, 0.4$, and 0.5) synthesized by Pramanik method are reported. The single phase formation of the ferrites was confirmed by XRD technique. The lattice parameter is found to increase with increase in Cu content. Average grain size, obtained from SEM micrographs, is found to increase with increase in Cu content. Dielectric parameters were measured as a function of frequency at room temperature as well as at higher temperatures. The variation in dielectric constant (ϵ') with temperature at four different fixed frequencies viz. 1 kHz, 10 kHz, 100 kHz, and 1 MHz was also studied. The room temperature dielectric constant (ϵ') and dielectric loss ($\tan \delta$) are found to decrease with increase in frequency. The ac conductivity (σ_{ac}) is found to increase with increase in the frequency.

© 2010 Elsevier B.V. All rights reserved.

1. Introduction

The field of spinel ferrites is well cultivated because of their various potential applications and the interesting physics involved in it [1–3]. Even after more than half of the century the scientist, researchers, technologist, and engineers are still excited in various types of bulk as well as nanocrystalline ferrite materials. The recent trend is focused on the doped ferrites prepared using various synthesis techniques with different cation concentrations which in turn affects the various properties like, electrical, dielectric, and magnetic behavior. Multilayer chip indicators (MLCIs) [3] are one of the important components for the latest electronic product used in cellular phones, video cameras, notebook computer, etc. because they are fabricated by putting alternate layers of ferrite and silver electrode. The magnetic and electrical properties of soft ferrites could be easily turned by incorporation and suitable addition of divalent or trivalent cations in the spinel structure. Therefore spinel ferrites become the important class of commercially available ferrites extensively used in microwaves and electrical industries [2] such as pulsed transformers, inductors, reflection coils, antennas, and modulators because of their high resistivity combined with useful ferromagnetic as well as dielectric constant behavior [3].

A recent literature survey on the structural and dielectric properties of various spinel nanocrystalline ferrites is discussed here in brief. Fayek et al. [4] have reported effect of Zn substitution on

dielectric properties of $\text{Cu}_{1-x}\text{Zn}_x\text{Ga}_{0.5}\text{Fe}_{1.5}\text{O}_4$ ferrite prepared by solid state method. Their results of frequency dependent dielectric loss ($\tan \delta$) behavior show relaxation spectra, where the authors determine relaxation time and the maximum frequency for the hopping mechanism. Sivakumar et al. [5] have concluded that the real part of the dielectric constant (ϵ') is found to be around 100 for milled MgFe_2O_4 (with 27 nm and 19 nm grain size), which are two orders of magnitude smaller than that of the bulk MgFe_2O_4 (micron size grains). The authors also observe anomalous behavior of dielectric constant (ϵ'), which has been explained based on the presence of both n-type and p-type charge carriers. Kaiser [6] has investigated the effect of Ni substitution on various properties of $(\text{Cu}_{0.8-x}\text{Zn}_{0.2}\text{Ni}_x)\text{Fe}_2\text{O}_4$ ferrites. Their electrical measurements at various compositions were investigated from room temperature up to 650 K in the frequency range (10^2 – 10^5 Hz). They conclude that the transition temperature (T_c) of $(\text{Cu}_{0.8-x}\text{Zn}_{0.2}\text{Ni}_x)\text{Fe}_2\text{O}_4$ increases with an increasing Ni concentration. Reddy et al. [7] studied the influence of copper substitution on structural and electrical properties of MgCuZn ferrites prepared by microwave sintering method. Their reported results reflect that, the lattice parameter (a) slowly increases, whereas the density sharply increases with increasing concentration of Cu ions in the MgCuZn ferrite. Ahmed et al. [8] and Ata-Allah and Fayek [9] have reported Cu substituted Ni, Zn, and Mn ferrites. Their results show strong influence of concentration of Cu substitution on frequency and temperature dependence dielectric properties like dielectric constant (ϵ') and dielectric loss ($\tan \delta$).

In the light of the literature [4–9] as discussed above, it is well known that the structural and the dielectric properties of ferrites

* Corresponding author. Tel.: +91 02024229369; fax: +91 02026999001.

E-mail address: milindbhandare@gmail.com (A.M. Shaikh).

Table 1
Data on variation of lattice constant, X-ray density, actual density, crystallite size, grain size and dielectric constant (at 1 kHz) of $\text{Ni}_{0.5-x}\text{Cu}_x\text{Zn}_{0.3}\text{Mg}_{0.2}\text{Fe}_2\text{O}_4$ ferrite samples (where $x=0, 0.1, 0.3$ and 0.5) with Cu-content.

	Lattice constant, a (Å)	X-ray density, gm/cm^3	Actual density, gm/cm^3	Crystallite size from XRD, nm	Grain size from SEM, μm	Dielectric constant (ϵ') at 1 kHz
0.0	8.40	5.082	3.45	35	0.28	146.47
0.1	8.41	5.488	3.88	37	0.41	131.19
0.3	8.42	6.289	4.65	44	0.70	99.25
0.5	8.44	7.090	4.84	45	0.82	84.15

are strongly dependent on method of synthesis, sintering temperature, chemical composition and grain structure or size [10]. Hence, the study of such properties at different frequencies, temperatures and chemical compositions may provide valuable information about the kind and amount of additives required to obtain high quality materials for practical applications. As a result, the study of electric and dielectric properties is equally important as those of magnetic properties from the applied fundamental research point of view. Many efforts [11–16] have been made to improve the basic properties of NiCuZn ferrite materials by substituting or adding various ions of different valence states depending on the applications of interest. Generally, the substitution of divalent or trivalent ions in the pure ferrites results in the modification of their structural, electrical and dielectric properties.

Mg–Cu–Zn ferrites are prominent magnetic materials for wide applications because of their high resistivity, high Curie temperature and environmental stability [17]. Also Liu et al. [18] have reported the effect of Mg containing ferrites composition is preferred to avoid the presence of divalent iron (to obtained high resistivity) and avoid the tendency of discontinuous grain growth which is an essential requirement to obtain dense ferrites. It is well reported recently [8,9,19,20] that the addition of Cu can effectively affects the structural, morphological and dielectric properties of spinel ferrites. Thus we expect that, Cu substitute in Ni–Mg–Zn ferrites may improve the structural, morphological and dielectric properties of the Ni–Zn–Mg ferrites. In the present work our prime aim is to study the successful synthesis of Cu substituted Ni–Mg–Zn ferrite using Pramanik method [21] and possible effects of Cu substitution on various properties of the Ni–Zn–Mg ferrite. We have also focused on the temperature dependent dielectric properties at fixed frequencies.

2. Experimental

The present samples are synthesized using Pramanik method [21] which consists of two steps. First, the stoichiometric amounts of AR Grade nickel nitrate $[\text{Ni}(\text{NO}_3)_2 \cdot 6\text{H}_2\text{O}]$, zinc nitrate $[\text{Zn}(\text{NO}_3)_2 \cdot 6\text{H}_2\text{O}]$, magnesium nitrate $[\text{Mg}(\text{NO}_3)_2 \cdot 6\text{H}_2\text{O}]$, copper nitrate $[\text{Cu}(\text{NO}_3)_2 \cdot 3\text{H}_2\text{O}]$ and iron nitrate $[\text{Fe}(\text{NO}_3)_3 \cdot 9\text{H}_2\text{O}]$ are mixed together with 10% aqueous solution of polyvinyl alcohol (PVA) and aqueous solution of sucrose (2 mol per metal ion). This solution is heated slowly at 200°C for 3 h in air atmosphere to form viscous liquid. The evaporation is accompanied by evolution of brown fumes of nitrogen dioxide (NO_2) due to decomposition mixture of nitrates. This distributes the cations throughout the polymer structure so that selective precipitation is prevented during the evaporation process. In the second step the precursor solution of metal nitrate–PVA–sucrose is evaporated completely to produce fluffy carbonaceous pyrolysed mass. The carbonaceous dry mass is calcined at 600°C for 3 h. The calcined ferrite powder is granulated using PVA as a binder and were uniaxially pressed at pressure of 5 ton/cm^2 for 5 min to produce pellet specimens having 10 mm diameter and 3 mm thickness. The specimens are finally sintered at 800°C for 4 h in air [22].

The crystallographic analysis of the samples was carried out by X-ray diffraction technique (XRD Model: Bruker D8 Advanced) using Cu K_α radiation (with $\lambda = 1.5406\text{ Å}$). The 2θ angle was varied from 20° to 80° . The microstructure of the samples was recorded using scanning electron microscope (SEM Model: JSM 6360A). The average grain size of the samples was estimated by lineal intercept method using the formula:

$$G_a = \frac{1.5L}{MN} \quad (1)$$

where L is the total test line length, M is the magnification, N is the total number of intercept.

The dielectric measurements were performed, at room temperature as well as at elevated temperature (30 – 600°C), at four fixed different frequencies viz. 1 kHz, 10 kHz, 100 kHz and 1 MHz, using LCR meter bridge (Model: HIOKY3532–50LCR). The dielectric constant (ϵ') was calculated using the relation:

$$\epsilon' = \frac{Cd}{\epsilon_0 A} \quad (2)$$

where C is the capacitance (in F), ϵ_0 is the permittivity of free space, d is the thickness (in m) and A is the cross-sectional area (in m^2) of the flat surface of the pellet.

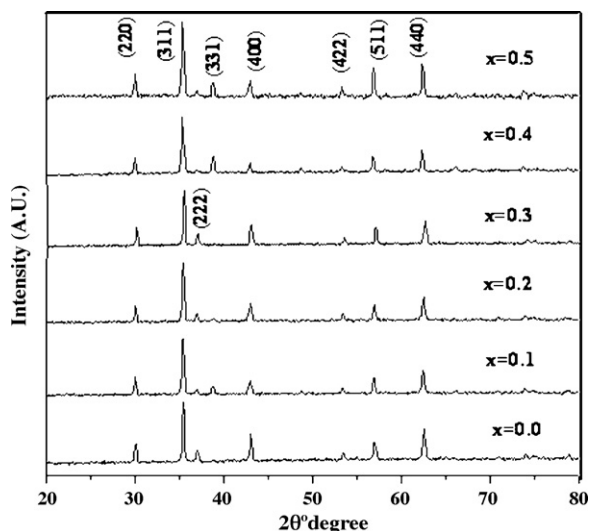


Fig. 1. XRD patterns of $\text{Ni}_{0.5-x}\text{Cu}_x\text{Zn}_{0.3}\text{Mg}_{0.2}\text{Fe}_2\text{O}_4$ ferrite samples (where $x=0.0, 0.1, 0.2, 0.3, 0.4$, and 0.5).

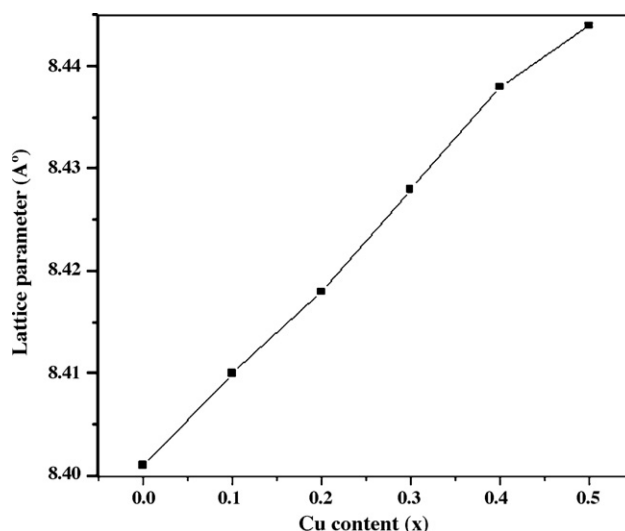


Fig. 2. Variation of lattice constant with Cu content of $\text{Ni}_{0.5-x}\text{Cu}_x\text{Zn}_{0.3}\text{Mg}_{0.2}\text{Fe}_2\text{O}_4$ ferrite samples (where $x=0.0, 0.1, 0.2, 0.3, 0.4$, and 0.5).

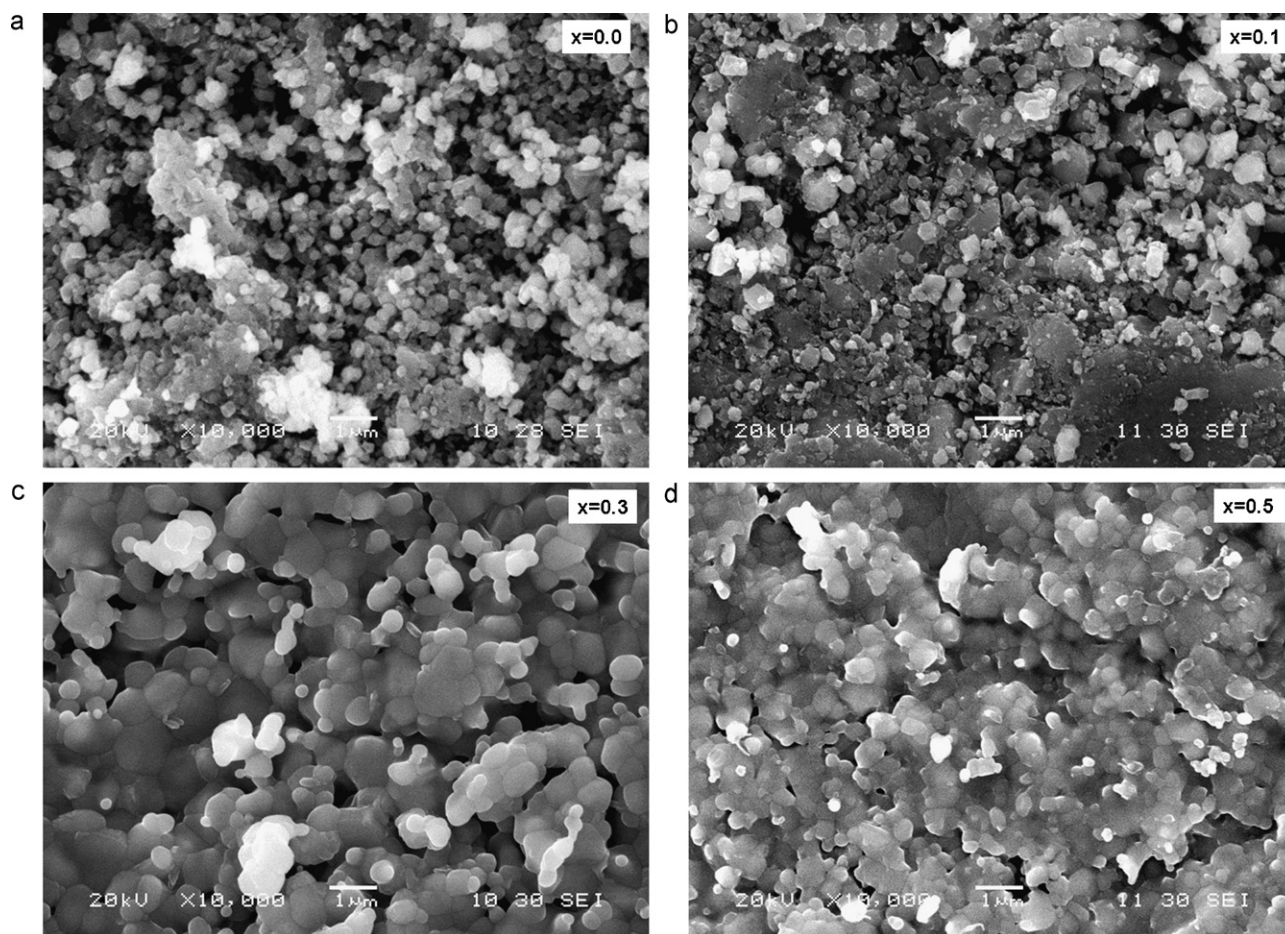


Fig. 3. Scanning electron micrographs of $\text{Ni}_{0.5-x}\text{Cu}_x\text{Zn}_{0.3}\text{Mg}_{0.2}\text{Fe}_2\text{O}_4$ ferrite samples (where $x=0.0, 0.1, 0.3$ and 0.5).

The ac conductivity of the samples was computed from dielectric parameters using the relation,

$$\sigma_{ac} = \epsilon' \epsilon_0 \omega \tan \delta \quad (3)$$

where ϵ' is the dielectric constant, ϵ_0 is permittivity of free space (8.854×10^{-12} F/m), ω is angular frequency and $\tan \delta$ is the loss tangent.

3. Results and discussion

The XRD patterns of the samples with $x=0.0, 0.1, 0.2, 0.3, 0.4$ and 0.5 are shown in Fig. 1. The patterns indicate well-defined peaks of crystalline FCC phase which confirm spinel cubic structure formation for the samples. No additional impurity reflections were observed ensuring the phase purity. The crystallite sizes of the studied samples ($x=0.0, 0.1, 0.3$ and 0.5) calculated using Debye–Scherrer formula [23] are listed in Table 1. Fig. 2 shows the variation of lattice constant with Cu content of the ferrite samples with $x=0.0, 0.1, 0.2, 0.3, 0.4$, and 0.5 . It is observed that the lattice constant increases linearly from 8.401 \AA for $x=0$ – 8.444 \AA for $x=0.5$ obeying Vegard's law. The increase in lattice constant is due to substitution of Cu^{2+} ions having larger ionic radius (0.72 \AA) than Ni^{2+} ions (0.69 \AA) [24]. Furthermore, substitution of Cu ions may cause migration of Fe^{3+} ions from A site to B site causing an overall expansion of the lattice.

Fig. 3 shows the SEM micrographs of the samples with $x=0.0, 0.1, 0.3$, and 0.5 . It is observed that majority of grains are spherical in shape. The SEM micrograph for $x=0$ shows well dispersed grains with identical shape and size. It is interesting to note that, as the amount of Cu^{2+} content increases, the nature of microstructure gets modulated. In the case of $x=0.1$ the grains are non identical in size and shape whereas for the case of $x=0.5$ the grains are agglomer-

ated. The average grain size calculated from Eq. (1) for different x is listed in Table 1. It is clear from Table 1 that, as the content of x increase the average grain size almost linearly increases. It suggests that, the substitution of Cu helps phase formation of spinel cubic lattice. It means that the temperature required for the phase formation of the ferrite with Cu doping is low as compared with the undoped ferrite. The synthesized samples possess large grain size due to high sintering temperature (i.e. 800°C for 4 h). Shrotri et al. [25] reported that one of the functions of copper is to decrease of sintering temperature. As in the present case, the sintering temperature and time of all the ferrite samples is same (i.e. 800°C for 4 h), the Cu doped samples shows high grain size as the compared to remaining samples. These results also suggest that addition of Cu enhances the grain growth process, which may due to the soft nature of Cu as compared to Ni.

Fig. 4(a) shows variation of dielectric constant for the samples with $x=0.0, 0.1, 0.3$ and 0.5 with frequency at room temperature. It is observed that, the dielectric constant is higher at lower frequencies and further it decreases with increase in frequency which is the normal behavior of dielectric constant. This behavior is attributed to space charge polarization due to inhomogeneous microstructure as well as mismatch in the electron exchange interaction between $\text{Fe}^{2+} \leftrightarrow \text{Fe}^{3+}$ ions which cannot follow the high alternating electric field [26]. It is also observed that the dielectric constant decreases with increase in Cu content. The substitution of Cu for Ni could modify the structural homogeneity which would cause a decrease in the degree of polarization [27].

Fig. 4(b) shows variation of $\tan \delta$ (for samples with $x=0.0, 0.1, 0.3$ and 0.5) as a function of frequency at room temperature. It is

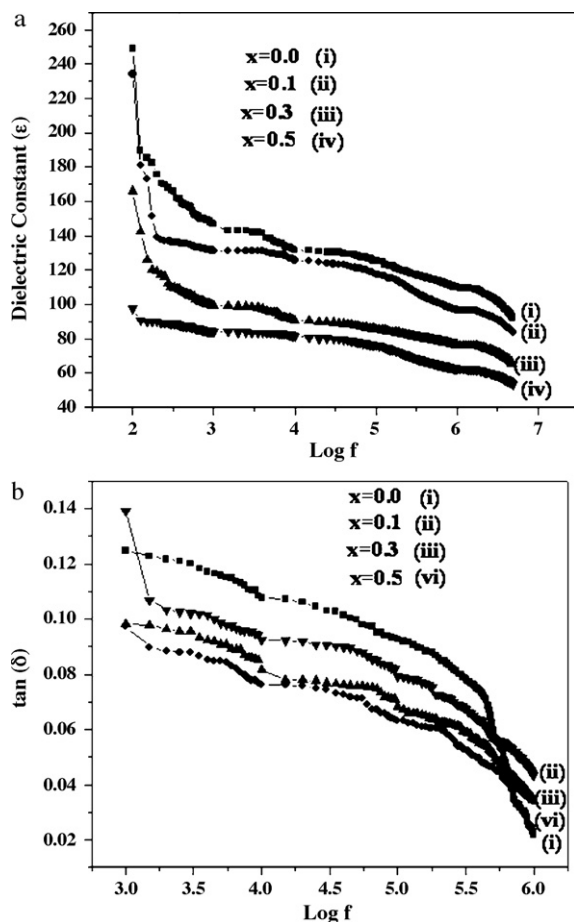


Fig. 4. (a) Variation of dielectric constant (ϵ') with frequency of $\text{Ni}_{0.5-x}\text{Cu}_x\text{Zn}_{0.3}\text{Mg}_{0.2}\text{Fe}_2\text{O}_4$ ferrite samples (where $x=0.0, 0.1, 0.3$ and 0.5). (b) Variation of dielectric loss tangent ($\tan \delta$) as a function of frequency of $\text{Ni}_{0.5-x}\text{Cu}_x\text{Zn}_{0.3}\text{Mg}_{0.2}\text{Fe}_2\text{O}_4$ ferrite samples (where $x=0.0, 0.1, 0.3$ and 0.5).

observed that $\tan \delta$ decreases continuously with increase in frequency. The high value of $\tan \delta$ at lower frequencies corresponds to high value of resistivity due to grain boundaries. Hence more energy is required for electron exchange between $\text{Fe}^{2+} \leftrightarrow \text{Fe}^{3+}$ ions resulting in high value of energy loss. However, in the higher frequency range, small amount of energy is needed for electron transfer between $\text{Fe}^{2+} \leftrightarrow \text{Fe}^{3+}$ ions resulting in small energy loss and low value of resistivity.

Fig. 5 shows variation of ac conductivity for the samples with $x=0.0, 0.1, 0.3$, and 0.5 with frequency at room temperature. It is observed that the ac conductivity increases with increase in frequency. The results are explained in terms of two regions of frequency: I-region (100–300 Hz) and II-region (300 Hz to 1.6 MHz). In the I-region grain boundaries are more active so that electron hopping probability between $\text{Fe}^{2+} \leftrightarrow \text{Fe}^{3+}$ ions is less, whereas in the II-region conducting grains become more active by promoting the hopping between $\text{Fe}^{2+} \leftrightarrow \text{Fe}^{3+}$ ions. The linearity in the II-region is attributed to small polaron type conduction [28]. Generally conduction in ferrites depends upon the hopping of electrons between $\text{Fe}^{2+} \leftrightarrow \text{Fe}^{3+}$ on octahedral site and also on the hopping of holes between Cu^{2+} and Cu^{1+} on tetrahedral sites. The frequency dependence of ac conductivity can be explained with the help of Maxwell–Wagner two-layer model for polycrystalline ferrites [29]. According to this model there are two layers formed in dielectric structure. The first layer consists of ferrite grains of fairly well conducting ferrous ions that is separated by thin layers of poorly conducting substance which forms grain boundary.

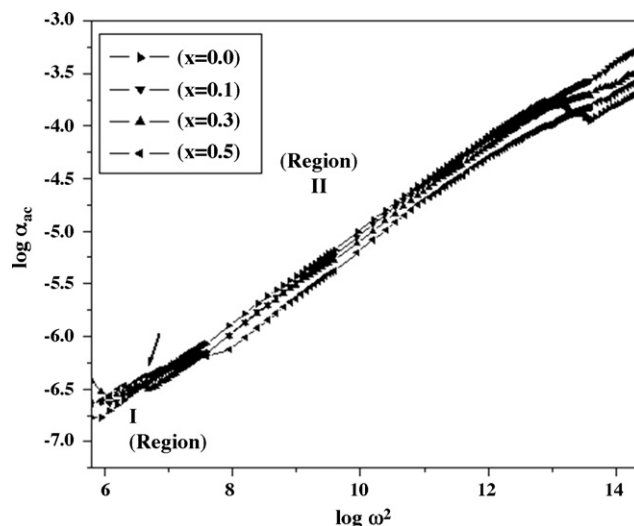


Fig. 5. Variation of ac conductivity with frequency of $\text{Ni}_{0.5-x}\text{Cu}_x\text{Zn}_{0.3}\text{Mg}_{0.2}\text{Fe}_2\text{O}_4$ ferrite samples (where $x=0.0, 0.1, 0.3$ and 0.5).

Fig. 6(a) shows variation of the dielectric constant (ϵ') for $x=0$ as a function of temperature. In the low temperature region (from 300 K to 635 K), it is observed that the magnitude of dielectric constant (ϵ') recorded at frequencies 1 kHz, 10 kHz, 100 kHz and 1 MHz

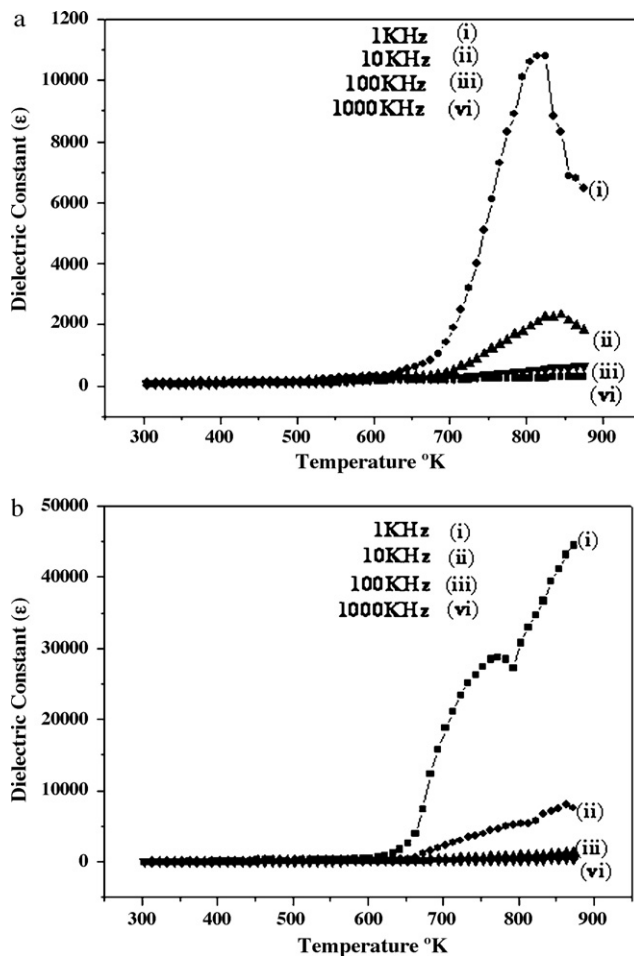


Fig. 6. (a) Variation of dielectric constant (ϵ') with temperature of $\text{Ni}_{0.5}\text{Zn}_{0.3}\text{Mg}_{0.2}\text{Fe}_2\text{O}_4$ ferrite samples. (b) Variation of dielectric constant (ϵ') with temperature of $\text{Cu}_{0.5}\text{Zn}_{0.3}\text{Mg}_{0.2}\text{Fe}_2\text{O}_4$ ferrite samples.

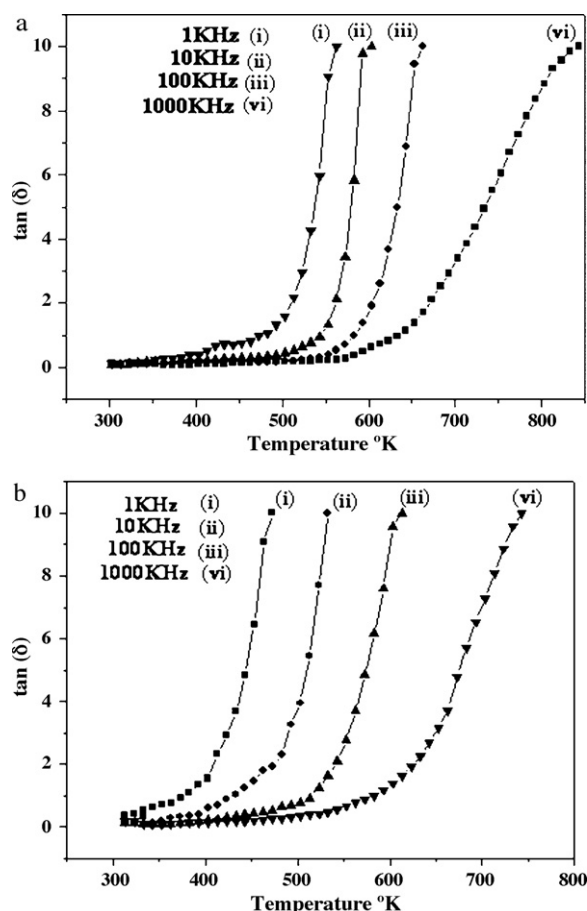


Fig. 7. (a) Variation of $\tan \delta$ with temperature of $\text{Ni}_{0.5}\text{Zn}_{0.3}\text{Mg}_{0.2}\text{Fe}_2\text{O}_4$ ferrite samples. (b) Variation of $\tan \delta$ with temperature of $\text{Cu}_{0.5}\text{Zn}_{0.3}\text{Mg}_{0.2}\text{Fe}_2\text{O}_4$ ferrite samples.

is almost constant. This can be explained on the basis of thermal agitation of dipole movement. In lower temperature region up to 635 K, the thermal energy is insufficient to free the localized dipoles to orient themselves in the direction of applied oscillating electric field. Above 635 K, the dielectric constant increases rapidly for frequencies 1 kHz and 10 kHz, whereas it increases slowly at frequency 100 kHz and almost remains constant at frequency 1 MHz. This can be attributed to the orientation of large number of dipoles in the direction of applied field due to sufficient amount of thermal agitation. The dielectric constant (ϵ') is observed to increase to a maximum value of (i) 10,790 recorded for 1 kHz and (ii) 2000 recorded for 10 kHz at 830 K, followed by decrease with further increase in temperature. This decrease in the dielectric constant above 830 K can be attributed to the magnetic phase transition of the sample from ferrimagnetic to paramagnetic phase. The magnetic transition temperature T_C for the sample ($x=0$) is reported [30] to be 830 K. The speculated change in the phase could modify the internal viscosity of the sample which leads to the more degree of freedom to the dipoles with increasing disorder in the system and hence decrease in dielectric constant.

The variation of dielectric constant with temperature for the sample with $x=0.5$ is shown in Fig. 6(b). It is observed that the temperature dependent dielectric constant follows the same path as observed in Fig. 6(a). Interestingly, the ferromagnetic to paramagnetic phase transition temperature is found to shift towards low temperature region, i.e. 773 K for $x=0.5$ as compared to $x=0$ sample. The shift in transition temperature may be attributed to the lower concentration of Ni, as it is substituted by Cu. Similar behav-

ior was also observed by Ahmad et al. [31] in case of lanthanum substituted Ni–Zn ferrites.

Fig. 7(a) and (b) shows the variation of $\tan \delta$ with temperature for the samples with $x=0$ and $x=0.5$, respectively, at four different fixed frequencies viz. 1 kHz, 10 kHz, 100 kHz, and 1 MHz. It is observed that as temperature increases $\tan \delta$ begins to increase until it attains a maximum value. Similar behavior was observed in case of zinc substituted magnesium rich manganese ferrites [32] and also in rare earth substituted Cu–Zn ferrites [33]. The gradual shift in loss tangent edge for samples $x=0$ and $x=0.5$ indicates that hopping mechanism is operative in this process. The frequency of hopping is approximately equal to the external applied electric field frequency [34].

4. Conclusions

X-ray diffraction patterns confirm the formation of cubic spinel phase without any additional impurity peaks indicating successful synthesis of all the ferrites using Pramanik method. The lattice constant (a) is found to increase with increase in copper content and is attributed to the larger ionic size of copper. Analysis of the SEM micrographs shows that, high content of Cu help for the formation of spinel phase at low sintering temperature. This concludes that, the high content of Cu poses large grain size as compared to undoped ($x=0$) sample. The room temperature dielectric constant and loss tangent ($\tan \delta$) are found to decrease with increase in Cu content over the measured frequency range. The observed phenomenon is attributed to the hopping of electrons between $\text{Fe}^{2+} \leftrightarrow \text{Fe}^{3+}$ ions as well as space charge polarization. The variation of ac conductivity (σ_{ac}) suggests that conduction is due to small polaron-hopping. Transition temperature (T_C) obtained from dielectric measurements are found to decrease with increase in Cu content.

Acknowledgments

MRB is thankful to U.G.C., WRO, Pune for financial support. Authors gratefully acknowledge the help received from Dr. V.L. Mathe, Department of Physics, University of Pune, Prof. B.A. Kamble, Principal, S.M. Joshi College, Hadapsar, Pune and Dr. P.S. Alegaonkar, College of Engineering, Pune (COEP).

References

- [1] A. Bayka, N. Kasapoglu, Y. Koseoglu, A.C. Basaran, H. Kavas, M.S. Toprak, Cent. Eur. J. Chem. 6 (1) (2008) 125–130.
- [2] C. Venkataraju, G. Sathishkumar, K. Sivakumar, J. Magn. Magn. Mater. 322 (2010) 230–233.
- [3] L. Yu, Y. Cui, X. Zhao, B. Zou, S.J. Feng, J. Magn. Magn. Mater. 301 (2006) 445–451.
- [4] M.K. Fayek, S.S. Ata-Allah, H.A. Zayed, M. Kaiser, S.M. Ismail, J. Alloys Compd. 469 (2009) 9–14.
- [5] N. Sivakumar, A. Narayanasamy, J.-M. Grenèche, R. Murugaraj, Y.S. Lee, J. Alloys Compd. 504 (2010) 395–402.
- [6] M. Kaiser, J. Alloys Compd. 468 (2009) 15–21.
- [7] M. Penchal Reddy, W. Madhuri, N. Ramamanoah Reddy, K.V. Siva Kumar, V.R.K. Murthy, R. Ramakrishna Reddy, Mater. Sci. Eng. C 30 (2010) 1094–1099.
- [8] M.A. Ahmed, M.K. El Nimr, A. Tawfik, A.M. El Hasab, J. Magn. Magn. Mater. 98 (1991) 33–36.
- [9] S.S. Ata-Allah, M.K. Fayek, Heper. Inter. 128 (2000) 467–469.
- [10] S.A. Mazen, S.F. Mansour, E. Dhahri, H.M. Zaki, T.A. Elmosalami, J. Alloys Compd. 470 (2009) 294–300.
- [11] C. Mukesh, C. Subhash, C. Dube, K. Mohanta, J. Electroceram. 16 (2006) 331–335.
- [12] P.K. Roy, J. Bera, J. Magn. Magn. Mater. 321 (2009) 247–251.
- [13] Z. Yue, J. Zhou, Z. Gui, L. Li, J. Magn. Magn. Mater. 264 (2003) 258–263.
- [14] Y. Fu, K. Pan, C. Lin, Mater. Lett. 57 (2002) 291–296.
- [15] V. Tsakaloudi, E. Eleftheriou, M. Stoukides, V. Zaspalis, J. Magn. Magn. Mater. 318 (2007) 58–64.
- [16] H. Su, H. Zhang, X. Tang, Y. Jing, Mater. Chem. Phys. 102 (2007) 271–274.
- [17] X.W. Qi, J. Zhou, Z.X. Yue, Z.L. Gui, L.T. Li, J. Magn. Magn. Mater. 251 (2002) 316–322.
- [18] D.M. Liu, J. Mater. Sci. 29 (1994) 1507–1513.
- [19] H. Su, H. Zhang, X. Tang, B. Liu, Z. Zhong, J. Alloys Compd. 475 (2009) 683–685.

- [20] H. Su, H. Zhang, X. Tang, Z. Zhong, Y. Jing, *Mater. Sci. Eng. B* 162 (2009) 22–25.
- [21] P. Pramanik, *Bull. Mater. Sci.* 22 (1999) 335–339.
- [22] M.M. Mallapur, P.A. Shaikh, R.C. Kamble, H.V. Jamadar, P.U. Mahamuni, B.K. Chougule, *J. Alloys Compd.* 479 (2009) 797–802.
- [23] B.D. Cullity, S.R. Stock, *Elements of X-Ray Diffraction*, 3rd ed., Prentice-Hall, Englewood Cliffs, NJ, 2001, p. 170.
- [24] T. Ahmed, I.Z. Rahman, M.A. Rhaman, *J. Mater. Process. Technol.* 797 (2004) 152–154.
- [25] J.J. Shrotri, S.D. Kulkarni, C.E. Deshpande, A. Mitra, S.R. Sainkar, P.S. Anil Kumar, S.K. Date, *Mater. Chem. Phys.* 59 (1999) 1–5.
- [26] K.K. Patankar, C.M. Kanamadi, B.K. Chougule, *Phys. Lett. A* 346 (2005) 337–341.
- [27] P.A. Jadhav, R.S. Devan, Y.D. Kolekar, B.K. Chougule, *J. Phys. Chem. Solids* 70 (2009) 396–400.
- [28] A. Alder, J. Feinleib, *Phys. Rev. B* 2 (1970) 3112–3134.
- [29] A.N. Patil, M.G. Patil, K.K. Patankar, R.P. Mahajan, S.A. Patil, *Bull. Mater. Sci.* 23 (2000) 447–452.
- [30] P.A. Shaikh, R.C. Kamble, A.V. Rao, Y.D. Kolekar, *J. Alloys Compd.* 482 (2009) 276–282.
- [31] M.A. Ahmed, E. Ateia, L.M. Salah, A.A. El-Gamal, *Mater. Chem. Phys.* 92 (2005) 310–321.
- [32] K.P. Thummer, H.H. Joshi, R.G. Kulkarni, *J. Mater. Sci. Lett.* 18 (1999) 1529–1532.
- [33] A.A. Sattar, S.A. Rahaman, *Phys. Stat. Sol. (a)* 200 (2003) 415–422.
- [34] W.H. Jung, H. Nakastugawa, E. Iguchi, *J. Solid State Chem.* 133 (1997) 466–472.